Transactions of the Materials Research Society of Japan 28 [3] 703-706 (2003)

Propagation Rate of a Fatigue Crack in Rectangular Aircraft Structural Panels Repaired with a Bonded FRP Composite Patch Containing a Piezoelectric Fiber Composite Actuator Layer

Shin-etsu Fujimoto and Hideki Sekine
Department of Aeronautics and Space Engineering, Tohoku University, Aoba-yama01, Aoba-ku, Sendai 980-8579, Japan
Fax: 81-022-217-6985, e-mail: hujimoto@plum.mech.tohoku.ac.jp
Fax: 81-022-217-6983, e-mail: sekine@plum.mech.tohoku.ac.jp

In this paper, we investigate the use of a piezoelectric fiber composite actuator layer to reduce the propagation rate of a fatigue crack in rectangular aircraft structural panels repaired with a bonded FRP composite patch. Finite element analysis is performed on the cracked rectangular aircraft structural panels repaired with a bonded FRP composite patch containing a piezoelectric fiber composite actuator layer under cyclic loading. Stress intensity ranges at the crack front are obtained, and propagation rates of the fatigue crack are estimated. Several shapes of fatigue crack are considered as numerical examples. The effects of the stacking position, size, and actuating segments of a piezoelectric fiber composite actuator layer on the propagation rate of the fatigue crack are examined.

Key words: Composite Patch Repair, Aircraft Structural Panel, Piezoelectric Fiber Composite Actuator Layer, Fatigue Crack, Propagation Rate

1. INTRODUCTION

Repair of cracked metallic aircraft structural panels using bonded FRP composite patches has been recognized as an efficient and cost-effective method to extend the service life of aging aircraft, and the application has been successfully demonstrated [1, 2]. Interest in the induced strain actuation of structures using piezoelectric materials has recently increased. Piezoelectric fiber composites have been developed for structural actuation applications [3]. Piezoelectric fiber composites offer the advantage of being both mechanically and piezoelectrically anisotropic. This anisotropy enables a selective means of actuating various modes within the plane of the structure and also allows modification of the properties of the composite actuator and its placement and orientation. These properties and this conformability enable piezoelectric fiber composites to be integrated into laminated composite structures.

This paper investigates the use of a piezoelectric fiber composite actuator layer to reduce the propagation rate of a fatigue crack in rectangular aircraft structural panels repaired with a bonded FRP composite patch under cyclic loading. We perform a finite element analysis on the repaired cracked rectangular aircraft structural panels. The stress intensity ranges at the crack front are obtained and the propagation rates of the fatigue crack are estimated. The effects of the stacking position, size, and actuating segments of a piezoelectric fiber composite actuator layer on the propagation rate of the fatigue crack are examined.

2. ANALYTICAL MODEL

We examine a cracked rectangular aircraft structural panel repaired with a bonded rectangular FRP composite patch containing a piezoelectric fiber composite actuator layer, as depicted in Fig. 1. The crack is located at the center of the panel, and a FRP composite patch

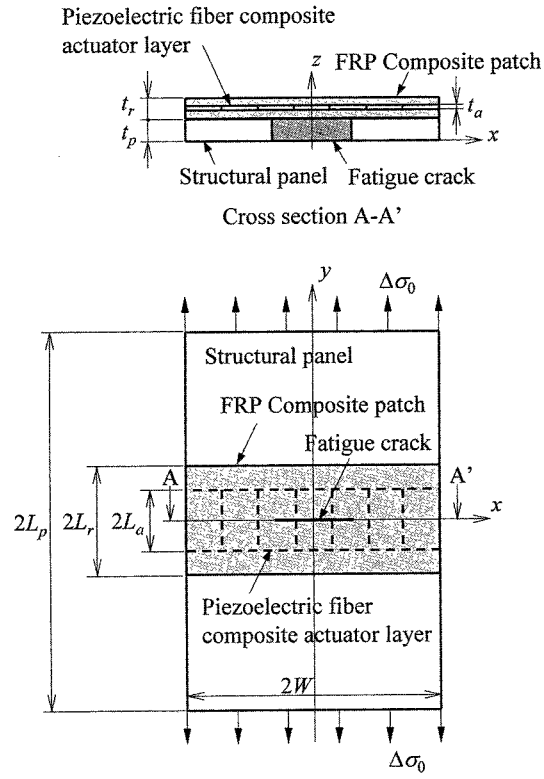

Fig.1. A cracked rectangular aircraft structural panel repaired with a bonded FRP composite patch containing a piezoelectric fiber composite actuator layer

containing a piezoelectric fiber composite actuator layer is bonded over the crack. A Cartesian coordinate system (x, y, z) is placed on the panel. The lengths of the cracked panel, FRP composite patch, and piezoelectric fiber composite actuator layer are $2L_p$, $2L_r$ and $2L_a$. They have the same widths of W. The thicknesses of the cracked panel, FRP composite patch, and piezoelectric fiber composite actuator layer are t_p, t_r, and t_a. The panel is subjected to cyclic applied stress with amplitude $\Delta\sigma_0$ at $y=\pm L_p$. The piezoelectric fiber composite actuator layer consists of seven pieces of piezoelectric fiber composite actuator with interdigitated electrodes [4], as illustrated in Fig. 2. Two plies of the piezoelectric fiber composite actuators are treated as a piezoelectric fiber composite actuator layer embedded in the FRP composite patch. The piezoelectric fiber composite actuator layer is operated only when the cracked structural panel is subjected to the maximum stress.

3. FINITE ELEMENT ANALYSIS

Finite element equations incorporating the piezoelectric load are given as follows:

$$\boldsymbol{K}\boldsymbol{u} = \boldsymbol{F} + \boldsymbol{F}_a \tag{1}$$

where $\boldsymbol{K}$ denotes the stiffness matrix, $\boldsymbol{u}$ represents the vector of nodal displacements, $\boldsymbol{F}$ is the applied force vector, and $\boldsymbol{F}_a$ is the induced actuation force vector. The strain induced by its actuation is expressed as

$$\Lambda_n = d_n \frac{V}{h_e} \tag{2}$$

where Λ_n is the induced strain, d_n is the piezoelectric material property, V is the applied voltage, and h_e is the distance between electrodes. Figure 3 contains a typical quarter model, in which eight-node isoparametric brick elements and eight-node singular elements modified from Akin's singular element with $O(r^{-\lambda})$ derivative singularity [5] are used. A total of 11,760 elements and 13,804 nodes are used in the model. The stress singularity at the tip of the small disbond at the intersection of the fatigue crack and the interface between the FRP composite patch and the structural panel is considered, as indicated in Fig. 4. The plane strain state is considered in the model and the eigen equation is derived by the method of Lekhnitskii [6]. The stress singularity is estimated by solving the eigen equation. The stress intensity factor is evaluated using the displacements at two points in the singular elements at the crack front [7].

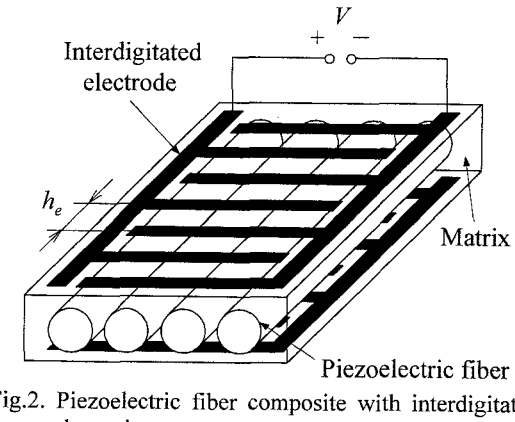

Fig.2. Piezoelectric fiber composite with interdigitated electrodes

4. RESULTS AND DISCUSSION

The repaired aircraft structural panel treated in this study is an aluminum panel (2024-T3). The FRP composite patch is a glass/epoxy, and the piezoelectric fiber composite actuator layer is a layer with PZT ceramic fibers embedded within an epoxy resin matrix. The FRP composite patch is a $[0/0/0/\pm45/0/0]_s$ laminate. The dimensions and material properties of the panel, FRP composite patch, and piezoelectric fiber composite actuator layer are given as follows.

(a) Structural panel: L_p=100mm, W=50mm, t_p=4.5mm, E=72.39GPa, ν=0.33.

(b) Lamina of FRP composite patch: L_r=25mm, W=50mm, t=0.23mm, E_{11}=44.12GPa, E_{22}=9.65GPa, G_{12}=4.13GPa, ν_{12}=0.36.

(c) Piezoelectric fiber composite actuator layer: L_a=25mm, 20mm, 15mm, 10mm, 5mm, t_a=0.34mm, E_{11}=30.53GPa, E_{22}=16.11GPa, G_{12}=5.5GPa, ν_{12}=0.36, d_{31}=381pm/V, d_{32}=−160pm/V.

The structural panel was subjected to cyclic applied stress with an amplitude of $\Delta\sigma_0$=45MPa and a stress

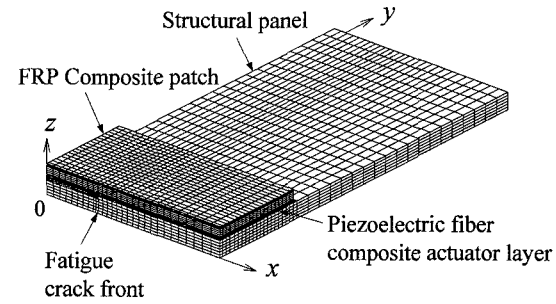

Fig.3. Finite element mesh

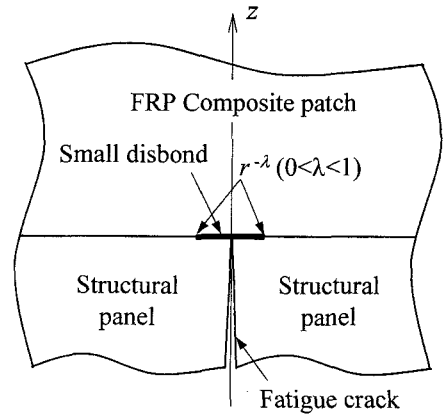

Fig.4. Small disbond at the intersection of the fatigue crack and the interface

ratio of R=0.1. The order of stress singularity λ was estimated by solving the eigen equation numerically as λ=0.5.

Three fatigue crack shapes were examined, as shown in Fig. 5. A finite element analysis was performed for several stacking positions of the piezoelectric fiber composite actuator layer and for each actuating segment, as illustrated in Fig. 6. The segments of the piezoelectric fiber composite actuator layer indicated in gray in the figure are the actuating ones. The induced strain can be obtained by applying an electric field to the piezoelectric fiber composite actuator layer. A positive or negative electric field on the piezoelectric fiber composite actuator layer causes in-plane tensile or compression strain with respect to the direction of the piezoelectric fiber orientation. The upper and lower limits of the electric field, used in numerical examples, were 1840V/mm and –790V/mm.

The crack propagation rates of the structural panel are estimated based on the following Paris relation:

$$\frac{da}{dN} = C(\Delta K)^n \tag{3}$$

where da/dN is the crack propagation rate, ΔK is the stress intensity factor range, and C and n are material constants obtained from experiments. The values used in the numerical examples were n=2.60 and C=1.15×10^{-6}(MPa·m$^{1/2}$)$^{-2.60}$mm/cycle.

Figure 7 provides the mean crack propagation rates along the crack front in the x direction for various stacking positions of the piezoelectric fiber composite actuator layer. The actuating segments used in this figure are Case A, and L_r=L_a. The value z_a is the stacking position of the piezoelectric fiber composite actuator layer normalized by the FRP composite patch thickness. For example, z_a=0.0 and 0.9 indicate cases in which the piezoelectric fiber composite actuator layer is located in the bonded interface and free surface of the FRP composite patch. The solid lines represent the results for Case E and the other lines are those for Case A. The mean crack propagation rates in the x direction differ according to the stacking position of the

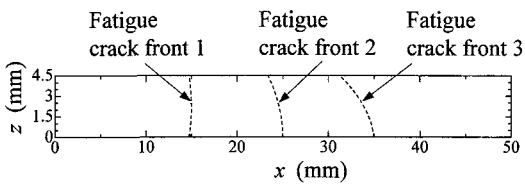

Fig.5. Shapes of fatigue crack front

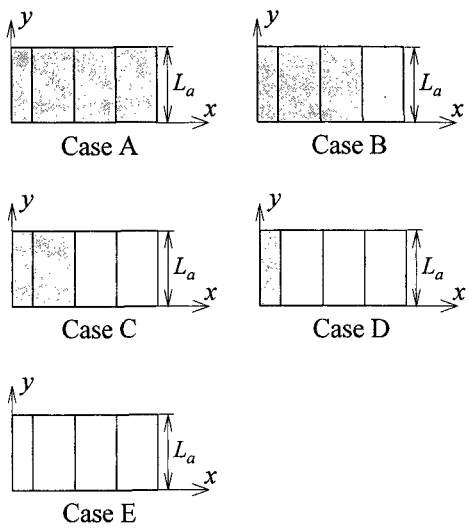

Fig.6. Actuating segments of piezoelectric fiber composite actuator layer

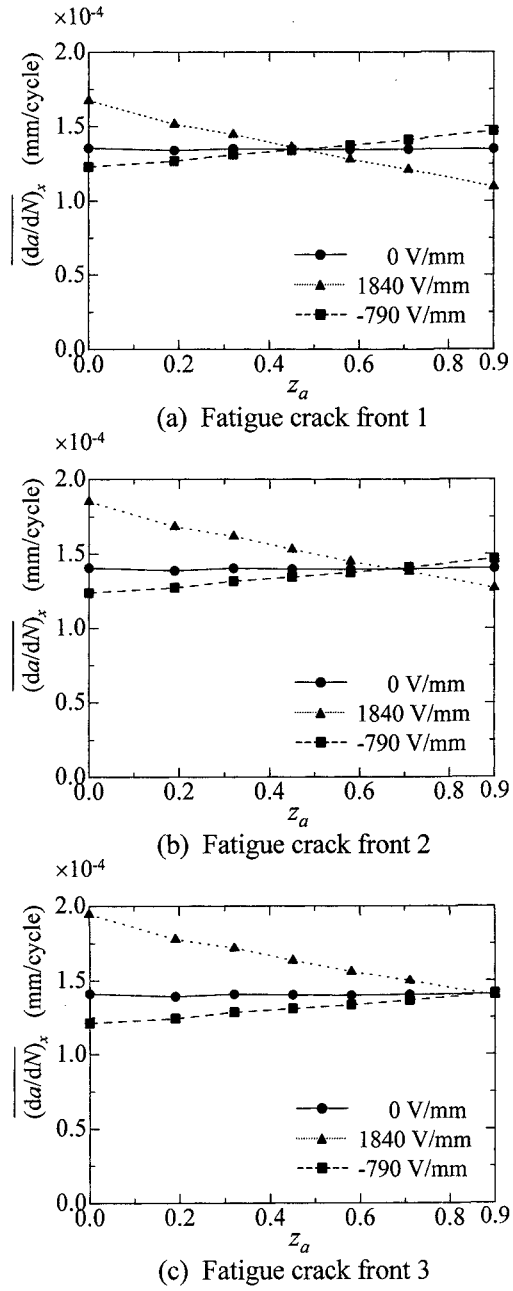

Fig.7. Mean crack propagation rates along the crack front in the x direction for various stacking positions of piezoelectric fiber composite actuator layer

piezoelectric fiber composite actuator layer. It is effective in Case A to have the piezoelectric fiber composite actuator layer located in the bonded interface of the FRP composite patch and the applied negative voltage to reduce the mean crack propagation rate along the crack front in the x direction. It is also useful to have the piezoelectric fiber composite actuator layer located in a free surface of the FRP composite patch and the applied positive voltage to reduce the mean crack propagation rate along the crack front in the x direction.

Various actuating segments and lengths L_a were considered to determine the effective size and actuating segments of the piezoelectric fiber composite actuator layer for several fatigue crack shapes. The mean crack propagation rates along the crack front in the x direction are listed in Tables I and II. The effective length of the piezoelectric fiber composite actuator layer is the length of the FRP composite patch and the effective actuating segments are Cases A and B when the stacking position of the piezoelectric fiber composite actuator layer is the bonded interface of the FRP composite patch. There were about 9%, 11%, and 14% reductions of the mean crack propagation rate in the x direction by actuation for the fatigue crack fronts 1, 2, and 3. Furthermore, the effective length of the piezoelectric fiber composite actuator layer is the length of the FRP composite patch and the effective actuating segment is Case A when the stacking position of the piezoelectric fiber composite actuator layer is the free surface of the FRP composite patch. There were about 18% and 9% reductions of the mean crack propagation rate in the x direction by actuation for the fatigue crack fronts 1 and 2. However, the effective length of the piezoelectric fiber composite actuator layer was 0.6 times as long as that of the FRP composite patch and the effective actuating segment is Case A for the fatigue crack front 3. There was about 3% reduction of the mean crack propagation rate in the x direction by actuation.

Table I. Mean crack propagation rates along the crack front in the x direction (Bonded interface, −790V/mm)

Fatigue crack front	L_d/L_r	$(\overline{da/dN})_x$ (mm/cycle)				
		Case A	Case B	Case C	Case D	Case E
1	1.0	1.229×10^{-4}	1.228×10^{-4}	1.239×10^{-4}	1.309×10^{-4}	1.354×10^{-4}
	0.8	1.254×10^{-4}	1.253×10^{-4}	1.260×10^{-4}	1.318×10^{-4}	1.355×10^{-4}
	0.6	1.279×10^{-4}	1.277×10^{-4}	1.281×10^{-4}	1.328×10^{-4}	1.356×10^{-4}
	0.4	1.306×10^{-4}	1.304×10^{-4}	1.306×10^{-4}	1.340×10^{-4}	1.360×10^{-4}
	0.2	1.334×10^{-4}	1.334×10^{-4}	1.333×10^{-4}	1.355×10^{-4}	1.365×10^{-4}
2	1.0	1.240×10^{-4}	1.248×10^{-4}	1.293×10^{-4}	1.377×10^{-4}	1.407×10^{-4}
	0.8	1.278×10^{-4}	1.283×10^{-4}	1.317×10^{-4}	1.387×10^{-4}	1.410×10^{-4}
	0.6	1.315×10^{-4}	1.317×10^{-4}	1.342×10^{-4}	1.398×10^{-4}	1.414×10^{-4}
	0.4	1.354×10^{-4}	1.354×10^{-4}	1.371×10^{-4}	1.411×10^{-4}	1421×10^{-4}
	0.2	1.388×10^{-4}	1.388×10^{-4}	1.396×10^{-4}	1.419×10^{-4}	1.425×10^{-4}
3	1.0	1.212×10^{-4}	1.243×10^{-4}	1.331×10^{-4}	1.382×10^{-4}	1.410×10^{-4}
	0.8	1.260×10^{-4}	1.281×10^{-4}	1.355×10^{-4}	1.395×10^{-4}	1.416×10^{-4}
	0.6	1.424×10^{-4}	1.409×10^{-4}	1.380×10^{-4}	1.321×10^{-4}	1.307×10^{-4}
	0.4	1.360×10^{-4}	1.367×10^{-4}	1.411×10^{-4}	1.430×10^{-4}	1.439×10^{-4}
	0.2	1.405×10^{-4}	1.407×10^{-4}	1.434×10^{-4}	1.443×10^{-4}	1.448×10^{-4}

Table II. Mean crack propagation rates along the crack front in the x direction (Free surface, 1840V/mm)

Fatigue crack front	L_d/L_r	$(\overline{da/dN})_x$ (mm/cycle)				
		Case A	Case B	Case C	Case D	Case E
1	1.0	1.096×10^{-4}	1.169×10^{-4}	1.252×10^{-4}	1.315×10^{-4}	1.349×10^{-4}
	0.8	1.141×10^{-4}	1.197×10^{-4}	1.263×10^{-4}	1.319×10^{-4}	1.351×10^{-4}
	0.6	1.186×10^{-4}	1.223×10^{-4}	1.271×10^{-4}	1.320×10^{-4}	1.351×10^{-4}
	0.4	1.238×10^{-4}	1.235×10^{-4}	1.288×10^{-4}	1.328×10^{-4}	1.356×10^{-4}
	0.2	1.305×10^{-4}	1.312×10^{-4}	1.324×10^{-4}	1.349×10^{-4}	1.366×10^{-4}
2	1.0	1.273×10^{-4}	1.329×10^{-4}	1.362×10^{-4}	1.381×10^{-4}	1.407×10^{-4}
	0.8	1.284×10^{-4}	1.328×10^{-4}	1.358×10^{-4}	1.382×10^{-4}	1.407×10^{-4}
	0.6	1.297×10^{-4}	1.328×10^{-4}	1.356×10^{-4}	1.386×10^{-4}	1.410×10^{-4}
	0.4	1.323×10^{-4}	1.340×10^{-4}	1.364×10^{-4}	1.396×10^{-4}	1.416×10^{-4}
	0.2	1.368×10^{-4}	1.374×10^{-4}	1.388×10^{-4}	1.412×10^{-4}	1.423×10^{-4}
3	1.0	1.397×10^{-4}	1.426×10^{-4}	1.388×10^{-4}	1.392×10^{-4}	1.408×10^{-4}
	0.8	1.378×10^{-4}	1.404×10^{-4}	1.381×10^{-4}	1.392×10^{-4}	1.408×10^{-4}
	0.6	1.363×10^{-4}	1.387×10^{-4}	1.380×10^{-4}	1.387×10^{-4}	1.414×10^{-4}
	0.4	1.367×10^{-4}	1.384×10^{-4}	1.392×10^{-4}	1.412×10^{-4}	1.426×10^{-4}
	0.2	1.394×10^{-4}	1.402×10^{-4}	1.415×10^{-4}	1.402×10^{-4}	1.394×10^{-4}

5. CONCLUSIONS

We investigated use of a piezoelectric fiber composite actuator layer to reduce the propagation rate of a fatigue crack in rectangular aircraft structural panels repaired with a bonded FRP composite patch under cyclic loading. We performed a finite element analysis on the repaired cracked rectangular aircraft structural panels. As a result, it was found that the mean crack propagation rates in the x direction differ according to the stacking position of the piezoelectric fiber composite actuator layer. The stacking position of the actuator layer should be either the bonded interface of the FRP composite patch and the applied negative voltage or the free surface of the FRP composite patch and the applied positive voltage to reduce the crack propagation rate when the piezoelectric fiber composite actuator layer is the same length as the FRP composite patch and all segments are actuated. The effective length of the piezoelectric fiber composite actuator layer for most cases is the length of the FRP composite patch, and the optimal effect is realized when all segments are actuated.

ACKNOWLEDGEMENT

This work was partly supported by Grant-in-Aid for Science Research (A) (2) No. 14205138 from the Japan Society for the Promotion of Science to HS.

REFERENCES

[1] A. A. Baker and R. Jones (Editors), "Bonded Repair of Aircraft Structures", Martinus Nijhoff Publishers, Dordrecht, The Netherlands (1988).
[2] A. A. Baker, *Composites*, **18**, 293-308(1987).
[3] N. W. Hagood and A. A. Bent, *AIAA Paper*, **93-1717**, 3625-3638 (1993).
[4] A. A. Bent and N. W. Hagood, *J. Intell. Mater. Syst. Struct.*, **8**, 903-919 (1997).
[5] J. E. Akin, *Int. J. Num. Meth. Engng.*, **10**, 1249-1259 (1976).
[6] S. G. Lekhnitskii, "Anisotropic Plates", Gordon and Breach (1968).
[7] W. S. Blackburn and T. K. Hellen, *Int. J. Num. Meth. Engng.*, **11**, 211-229 (1977).

(Received December 21, 2002; Accepted Febuary 21, 2003)